Assessing the CO_2 concentration at the surface of photosynthetic mesophyll cells

Marquez, Diego; Stuart-Williams, Hilary; Cernusak, Lucas A.; Farquhar, Graham D.

DOI:
10.1111/nph.18784

Document Version
Publisher's PDF, also known as Version of record

Citation for published version (Harvard):
Marquez, D, Stuart-Williams, H, Cernusak, LA & Farquhar, GD 2023, 'Assessing the CO_2 concentration at the surface of photosynthetic mesophyll cells', *New Phytologist*, vol. 238, no. 4, pp. 1446-1460. https://doi.org/10.1111/nph.18784

Research

New Phytologist

Assessing the CO_2 concentration at the surface of photosynthetic mesophyll cells

Diego A. Márquez[1], Hilary Stuart-Williams[1], Lucas A. Cernusak[2] and Graham D. Farquhar[1]

[1]Research School of Biology, Australian National University, Canberra, ACT 2601, Australia; [2]College of Science and Engineering, James Cook University, Cairns, Qld 4878, Australia

Author for correspondence:
Graham D. Farquhar
Email: graham.farquhar@anu.edu.au

Received: *18 July 2022*
Accepted: *21 January 2023*

New Phytologist (2023) **238:** 1446–1460
doi: 10.1111/nph.18784

Key words: abaxial, adaxial, gas exchange, gas exchange parameters, leaf internal CO_2 concentration, mesophyll conductance.

Summary

- We present a robust estimation of the CO_2 concentration at the surface of photosynthetic mesophyll cells (c_w), applicable under reasonable assumptions of assimilation distribution within the leaf. We used *Capsicum annuum*, *Helianthus annuus* and *Gossypium hirsutum*as model plants for our experiments.
- We introduce calculations to estimate c_w using independent adaxial and abaxial gas exchange measurements, and accounting for the mesophyll airspace resistances.
- The c_w was lower than adaxial and abaxial estimated intercellular CO_2 concentrations (c_i). Differences between c_w and the c_i of each surface were usually larger than 10 μmol mol^{-1}. Differences between adaxial and abaxial c_i ranged from a few μmol mol^{-1} to almost 50 μmol mol^{-1}, where the largest differences were found at high air saturation deficits (ASD). Differences between adaxial and abaxial c_i and the c_i estimated by mixing both fluxes ranged from −30 to +20 μmol mol^{-1}, where the largest differences were found under high ASD or high ambient CO_2 concentrations.
- Accounting for c_w improves the information that can be extracted from gas exchange experiments, allowing a more detailed description of the CO_2 and water vapor gradients within the leaf.

Introduction

Quantifying the intercellular CO_2 concentration in the airspace of the leaf is key to interpreting and understanding physiological traits and genetic variation of photosynthesis. In practice, it is known that the [CO_2] in the leaf airspace cannot be completely uniform (Parkhurst, 1994) except for the trivial case where there is no CO_2 uptake by, or release from the leaf. There is no method or technique for measuring CO_2 concentrations within the leaf directly, and thus we estimate [CO_2] using Fick's law for gas diffusion. The convention equates intercellular CO_2 concentration in the airspace of the leaf (c_i; list of abbreviations in Table 1) to the [CO_2] calculated using 1 : 1.6 times the estimated conductance to H_2O from the internal airspace to the atmosphere. The value 1.6 comes from the ratio of H_2O diffusivity in air to CO_2 diffusivity in air (Cowan, 1972). This calculation assumes that the airspaces within the leaf are uniformity saturated with water vapor at the leaf temperature measured on its surfaces (w_{sat}), and then that the internal water vapor mole fraction in the substomatal cavity (w_i) and the atmospheric water vapor mole fraction (w_a) may be used to represent the gradient that drives the exchange (Gaastra, 1959). Therefore, c_i is expected to be the [CO_2] in the substomatal cavity or nearby (Moss & Rawlins, 1963), because it is typically assumed that $w_i = w_{sat}$.

Thus, hypostomatous leaves have c_i estimated at the stomatous surface and amphistomatous leaves have adaxial and abaxial c_i. Parkhurst (1994) urges that distinction be made between [CO_2] in the adaxial and abaxial substomatal cavities and that CO_2 gradients exist in the leaf internal airspace. Over the range of CO_2 concentration between the surfaces, there must be a minimum CO_2 concentration that drives the gradient inward toward the mesophyll cell walls (c_w) from the adaxial and abaxial surfaces. The inclusion of c_w accounting for the CO_2 gradients in our calculations would allow us to subtract the internal airspace resistance, thus obtaining a more accurate estimate of the chloroplast-based traits. For instance, the CO_2 conductance between the mesophyll airspace and the stroma within the chloroplast, the mesophyll conductance to CO_2, is usually calculated using isotope discrimination techniques (Holloway-Phillips *et al.*, 2019) or chlorophyll fluorescence (Harley *et al.*, 1992) in conjunction with gas exchange measurements, relying on the precision of c_i calculations. The commonly used model for photosynthetic biochemistry (Farquhar *et al.*, 1980) relates its parameters to the CO_2 concentration in the chloroplast, the estimation of which relies on the c_i estimate and calculated mesophyll conductance to CO_2 (Sharkey *et al.*, 2007). The more subtle interpretations, for example of glycine and serine removal from the photorespiratory pathway (Busch *et al.*, 2020), are even more demanding on the c_i precision. Furthermore, the precision of intercellular CO_2 concentration determination is critical for discussing topics such as the Kok effect (Farquhar & Busch, 2017) and CO_2 concentration gradients in the mesophyll airspace (Parkhurst *et al.*, 1988;

Table 1 List of abbreviations and subscripts used in the text.

Abbreviation	Name
A	Net CO_2 assimilation rate
A_s	Net CO_2 assimilation rate through the stomata
ASD	Air saturation deficit (saturated air at this temperature–w_a)
c_a	CO_2 concentration in the atmosphere
c_i	CO_2 concentration in the substomatal cavity
$c_{i\text{-}Mix}$	c_i estimated using the combined gas fluxes
c_s	CO_2 concentration at the surface of a leaf
c_w	CO_2 concentration at the surface of mesophyll cells
E	Transpiration rate
g_{cw}	Cuticular conductance to H_2O
g_m	Mesophyll conductance to CO_2
g_{sw}	Stomatal conductance to H_2O
J_a	Electron transport rate
L	Length of gaseous paths from c_i to c_w
l	Tour on L path
m	Rate of change of photosynthetic uptake with x (du/dx)
PAR	Photosynthetically active radiation
$r(l)$	Cumulative resistance to CO_2 diffusion
r_{bc}	Boundary layer resistance to CO_2 diffusion
R_d	Dark respiration rate
R_{ias}	Total mesophyll airspace resistance to CO_2 diffusion
r_{ias}	Adaxial or abaxial internal airspace resistance to CO_2 diffusion
r_{sc}	Stomatal resistance to CO_2 diffusion
T	Mesophyll thickness
TPU	Triose phosphate utilization
$u(l)$	Cumulative photosynthetic uptake
V_{cmax}	Maximum carboxylation rate
VPD	Vapor pressure difference (w_{sat}–w_a) × Atmospheric pressure
w_a	Water vapor concentration in the atmosphere
w_i	Water vapor concentration in the substomatal cavity
w_s	Water vapor concentration at the surface of a leaf
w_{sat}	Saturated water vapor concentration at the leaf temperature
x	Transect x perpendicular to the leaf surface ($x = l/L$)
Δc_i	Difference between adaxial and abaxial c_i ($\Delta c_i = c_{i\text{-}ad}$–$c_{i\text{-}ab}$)
Δc_{Mix}	Difference between $c_{i\text{-}Mix}$ and c_i ($\Delta c_{Mix} = c_{i\text{-}Mix}$–$c_{i\text{-}ad}$ or $\Delta c_{Mix} = c_{i\text{-}Mix}$–$c_{i\text{-}ab}$)
Δc_{MW}	Difference between $c_{i\text{-}Mix}$ and c_w ($\Delta c_{MW} = c_{i\text{-}Mix}$–$c_w$)
Δc_w	Difference between the c_w estimated using different m values ($\Delta c_w = c_w(-0.31)$–$c_w(m)$)
Θ	Mean value for the proportion of A_s added with the walk in L
$\theta(x)$	Proportional photosynthetic uptake per unit of length
$\rho(l)$	Resistance per unit of length
$\upsilon(l)$	Photosynthetic uptake per unit of length
Subscript -ab	The abaxial face of the leaf
Subscript -ad	The adaxial face of the leaf

Parkhurst, 1994). We propose that improved estimates of c_w be used for calculations of photosynthetic biochemistry, mesophyll conductance, etc., minimizing the uncertainty of estimating c_i from the mixing of adaxial and abaxial fluxes.

Independent measurement of adaxial and abaxial gas exchange was once more commonly used (see Jarvis & Slatyer, 1966, Jones & Slatyer, 1972; Wong *et al.*, 1985b) to estimate adaxial and abaxial c_i; nowadays, in typical gas exchange measurements, gases from the upper and lower cuvettes are mixed assuming that the action does not affect the estimates. The widely used equations derived by von Caemmerer & Farquhar (1981) were based on a single leaf surface; nevertheless, they are usually used assuming that they can be applied directly to gas exchange measurements mixing adaxial and abaxial leaf gas exchange. The improved theory for calculating leaf gas exchange presented by Márquez *et al.* (2021a), was also based on a single leaf surface. Once the flows are mixed, the true adaxial and abaxial flux contributions are unknown. Thus, it has been common practice to treat c_i as the [CO_2] in a virtual substomatal cavity, calculated from the mix of both fluxes. Even though this practice has been common, there is not much information about its impact on the estimates of gas exchange parameters.

Here, we present a set of equations to estimate the CO_2 concentration that provides the sink for the fluxes inward from the adaxial and abaxial sides of the leaf (c_w), using independent measurements of adaxial and abaxial gas exchange. We argue that c_w is essentially the lumped parameter representing the CO_2 concentration at the surface of photosynthetic mesophyll cells. Additionally, we evaluate the actual values of adaxial and abaxial w_s, c_s, g_{sw} and c_i because, consciously or not, it is implicitly assumed with common gas exchange devices and calculations that the differences between adaxial and abaxial gas exchange parameters (w_s, c_s, g_{sw}, and c_i) are negligible. We hypothesize that this is incorrect and examine the errors inherent in mixing the adaxial and abaxial fluxes, explore their impact, and identify ranges of errors under different experimental conditions.

Theory of the model

In a photosynthetically active leaf, the CO_2 that has entered through the stomatal pores will move toward chloroplasts in the mesophyll cells, where the CO_2 concentration is lower due to the active rubisco CO_2 fixation. Mesophyll cells are the sink of CO_2 and thus the CO_2 concentrations surrounding them are the lowest in the leaf airspace. In the path from the substomatal cavity to the chloroplast, the CO_2 must diffuse through the gaseous phase of the mesophyll airspace and then through the liquid phase at the surface of the cell wall to the chloroplast stroma (detailed analysis of these paths can be found in Evans & von Caemmerer, 1996, Evans *et al.*, 2009; Evans, 2021; Mizokami *et al.*, 2022). The conductance offered in the latter liquid path is usually referred to as mesophyll conductance (g_m) and estimated assuming that the resistance and gradient in the airspace are negligible. Some general characteristics of these two phases in the path are: the resistivity (reciprocal of conductivity) to CO_2 diffusion through the liquid phase is 10 000 times larger than through the gaseous phase; and the thickness of the liquid phase is a couple of μm while the thickness of the leaf is *c.* 100 to 200 μm or more. Thus, the total resistance of the liquid phase path is about two orders of magnitude greater than the whole gas-phase resistance in the mesophyll airspace from adaxial to abaxial substomatal cavities (R_{ias}). However, the diffusion of CO_2 through the liquid path is aided by the diffusion of bicarbonate towards the site of rubisco in C_3 plants and the activity of the enzyme carbonic anhydrase, in a process called facilitated transfer (Enns, 1967; Cowan, 1986). Carbonic anhydrase interconverts dissolved CO_2

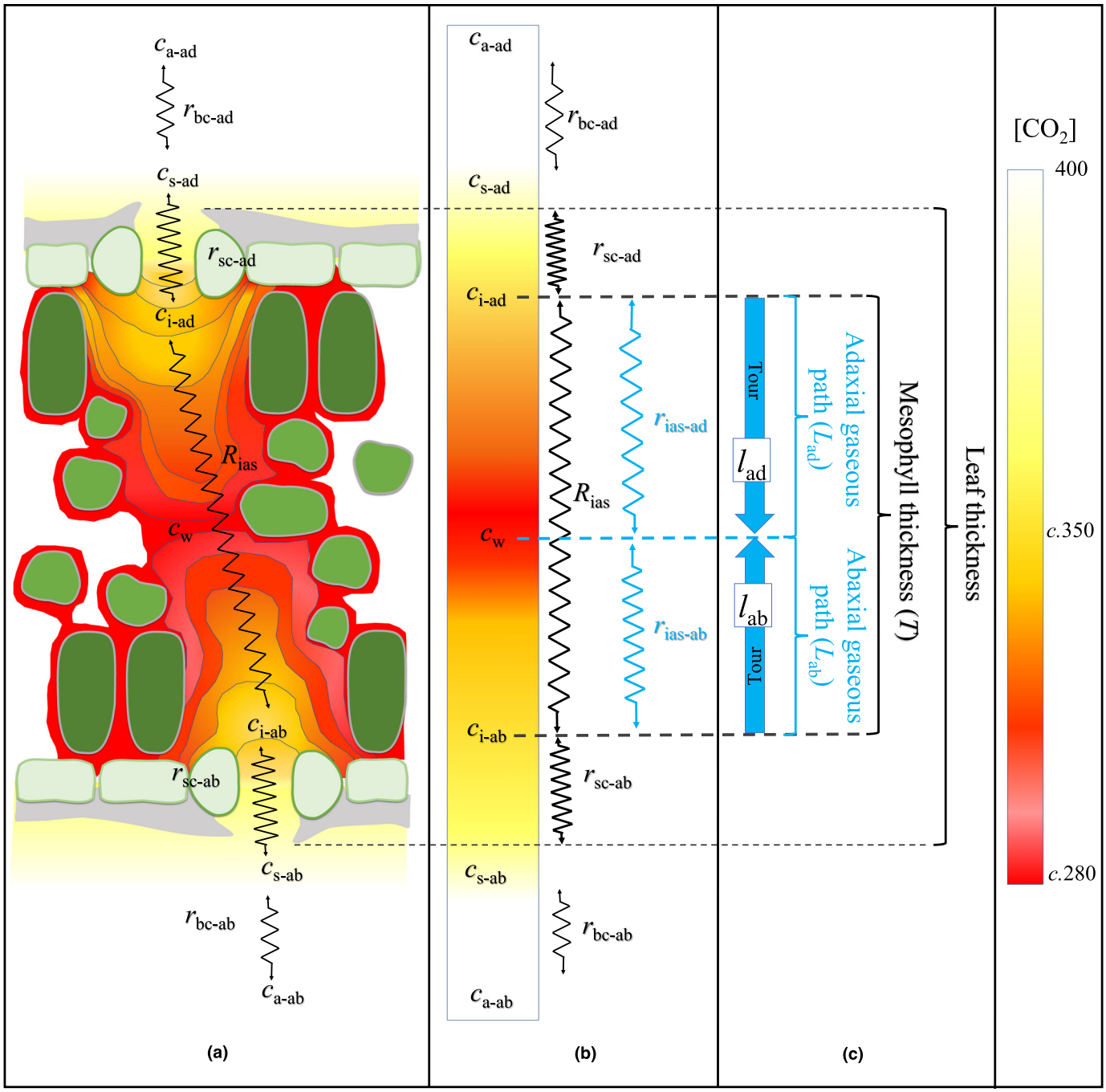

Fig. 1 Diagram of CO_2 concentration within a photosynthetically active leaf. (a) 2-D representation of the expected CO_2 distribution within an amphistomatous leaf, (b) 1-D representation of the CO_2 concentration and resistances involved in the model, and (c) representation of the adaxial and abaxial transects in the model. c_a is the CO_2 concentration in the atmosphere, c_s is the CO_2 concentration at the surface of a leaf, c_i is the CO_2 concentration in the substomatal cavity, c_w is the CO_2 concentration at the surface of mesophyll cells, r_{bc} is the boundary layer resistance to CO_2 diffusion, r_{sc} is the stomatal resistance to CO_2 diffusion, R_{ias} is the total mesophyll airspace resistance to CO_2 diffusion, r_{ias} is the internal airspace resistance to CO_2 diffusion, ad and ab subscripts stand for adaxial and abaxial, respectively.

and bicarbonate with the net effects that CO_2 is converted into bicarbonate near the plasma membrane, and bicarbonate is converted into CO_2 near rubisco (Raven & Glidewell, 1981). This effectively increases by one order of magnitude the amount of CO_2 transported, bringing the liquid phase path resistance down to only one order of magnitude larger than the whole gas-phase. Therefore, the CO_2 concentration drawdown in the gas phase is expected to be in the order of 10 μmol mol^{-1} and the CO_2 concentrations surrounding the mesophyll cells must be roughly similar, except for the few cells next to the stomatal cavity (Fig. 1a).

We can place c_w in a one-dimensional model of resistances to CO_2 diffusion between the adaxial and abaxial c_i, including R_{ias} and accounting for the fluxes of both sides of the leaf (Fig. 1b).

The gaseous paths from adaxial and abaxial c_i to c_w (L_{ad} and L_{ab}) meet at some point in the mesophyll airspace such that:

$$T = L_{ad} + L_{ab} \quad \text{Eqn 1}$$

where T is the mesophyll thickness (Fig. 1c). Then, each path (l_{ad} and l_{ab}) from c_i ($l = 0$) towards the interior of the leaf perpendicular to the leaf surface is completed at their respective L. The tortuosity in the mesophyll gaseous path (τ) depends on the section of the walk such that it is $\tau(l)$, and similarly for the light intensity $I(l)$, and biochemical activity $b(l)$. Thus, the resistance per unit of length (ρ) depends on τ, $\rho(\tau)$, and the photosynthetic uptake per unit of length (υ) depends on I and b, $\upsilon(I, b)$. Then, ρ and υ can be written as functions of l, $\rho(l)$ and $\upsilon(l)$; and for each side of the leaf, we describe a function $r(l)$ that is the cumulative resistance to CO_2 diffusion along the path

$$r(l) = \int_0^l \rho(k)\mathrm{d}k \quad \text{Eqn 2}$$

where k is a dummy variable and another function $u(l)$ that is the cumulative photosynthetic uptake along the path as

$$u(l) = \int_0^l \upsilon(k)\mathrm{d}k \quad \text{Eqn 3}$$

From gas exchange measurements, we know the net CO_2 assimilation through the stomata (A_s) and so

$$A_s = u(L) = \int_0^L \upsilon(k)\mathrm{d}k \quad \text{Eqn 4}$$

We can independently estimate the total mesophyll airspace resistance to CO_2 in the leaf (R_{ias}; see Materials and Methods section for details) and as R_{ias} occurs in the whole thickness of the mesophyll (T) we obtain

$$R_{ias} = r(T) = \int_0^T \rho(k)\mathrm{d}k \quad \text{Eqn 5}$$

R_{ias} is the sum of the adaxial (-ad) and abaxial (-ab) internal airspace resistances to CO_2 diffusion,

$$R_{ias} = r_{ias-ad} + r_{ias-ab} \quad \text{Eqn 6}$$

where $r_{ias\text{-}ad}$ and $r_{ias\text{-}ab}$ coincide at the minimum CO_2 concentration within the leaf airspace near the cell walls of photosynthetically active mesophyll cells (c_w; Fig. 1b). Then for each side

$$r_{ias} = r(L) = \int_0^L \rho(k)\mathrm{d}k \quad \text{Eqn 7}$$

All the CO_2 molecules cross through $l = 0$, but the CO_2 flux along L varies with the CO_2 consumption along the path. In a section of the path from 0 to l, we can describe the infinitesimal drawdown $\delta c(l)$ in CO_2 concentration associated with an infinitesimal increase δl at l and hence an increase in resistance of $(\mathrm{d}r(l)/\mathrm{d}l)\,\delta l$ as a function of $u(l)$ and $\rho(l)$ as

$$\delta c(l) = u(l)\rho(l)\delta l \quad \text{Eqn 8}$$

Integrating from 0 to l

$$\int_{c_i}^{c_l} \mathrm{d}c = \int_0^l \rho(k)u(k)\mathrm{d}k$$
$$c_i - c_l = \int_0^l \rho(k)u(k)\mathrm{d}k \quad \text{Eqn 9}$$

and then from Eqn 3

$$c_i - c_l = \int_0^l \rho(k)\int \upsilon(k)\mathrm{d}k\mathrm{d}k \quad \text{Eqn 10}$$

The forms of equations $\rho(l)$ and $\upsilon(l)$ are unknown but as $u(L) = A_s$, we can write a cumulative distribution function for $u(l)$ representing the changes in the photosynthetic uptake rate with the walk in L,

$$u(l) = \int_0^l \upsilon(k)\mathrm{d}k = A_s\int_0^l \theta(k)\mathrm{d}k \quad \text{Eqn 11}$$

where θ represents the ratio $\upsilon(l) : A_s$ and $\int\theta(k)\mathrm{d}k$ is the proportion of A_s added within the walk ($u(l)/A_s$) taking values from 0 to 1. In like manner, $r(L) = r_{ias}$ and thus we can write a cumulative distribution function for $r(l)$,

$$r(l) = \int_0^l \rho(k)\mathrm{d}k = r_{ias}\int_0^l \varphi(k)\mathrm{d}k \quad \text{Eqn 12}$$

where φ represents the ratio $\rho(l) : r_{ias}$ and $\int\varphi(k)\mathrm{d}k$ is the proportion of r_{ias} added within the walk ($r(l)/r_{ias}$) taking values from 0 to 1.

Substituting Eqns 11 and 12 in Eqn 10 we have

$$c_i - c_l = r_{ias}A_s\int_0^l \varphi(k)\int \theta(k)\mathrm{d}k\mathrm{d}k \quad \text{Eqn 13}$$

Here, we consider the resistance to CO_2 diffusion as constant per unit of length in L, $\rho(l) = r_{ias}/L$ or $\varphi(l) = 1/L$, and so Eqn 13 becomes

$$c_i - c_l = A_s r_{ias}\frac{1}{L}\int_0^l \int \theta(k)\mathrm{d}k\mathrm{d}k$$
$$c_i - c_l = \frac{A_s r_{ias}}{L}\Theta(l) \quad \text{Eqn 14}$$

where Θ is the double integral on the right-hand side of Eqn 14. Note that Θ has units of length, l, and $\int\theta(k)\mathrm{d}k$ is a function. Thus, to find the CO_2 concentration at l,

$$c_l = c_i - \frac{r_{ias} A_s}{L} \Theta(l) \quad \text{Eqn 15}$$

The length of each L is unknown but we know that l walks on L, so we represent the CO_2 path as a transect x perpendicular to the leaf surface such that $x = l/L$. Then, the transect moves from $x = 0$ to 1 where $x = 0$ is in the substomatal cavity and $x = 1$ is at c_w (Fig. 1c). Adapting Eqns 2–15 for the transect x results in

$$c_x = c_i - r_{ias} A_s \int_0^x \int \theta(k) \mathrm{d}k \mathrm{d}k \quad \text{Eqn 16}$$
$$c_x = c_i - r_{ias} A_s \Theta(x)$$

Eqn 16 in the case of $x = 1$ ($l = L$) yields

$$c_w = c_i - r_{ias} A_s \Theta(1) \quad \text{Eqn 17}$$

In general, the form of $\int \theta(k)\mathrm{d}k$ is unknown, and factors such as light quality may affect the form of $\theta(x)$ (see Vogelmann & Evans, 2002), but there is evidence of an almost linear decrease in the photosynthetic uptake from the stomatal cavity inward to the interior of the mesophyll (see Evans & Vogelmann, 2003). Thus, the shape of $\theta(x)$ would be close to a linear function and $\int \theta(k)\mathrm{d}k$ to a quadratic function. In practice, $\theta(x)$ could adopt any form to generate a desired shape for the proportional cumulative photosynthetic uptake, $\int \theta(k)\mathrm{d}k$. We represent $\theta(x)$ by a linear equation $\theta(x) = m(x - 0.5) + 1$, where m is the rate of change of photosynthetic uptake with x ($\mathrm{d}v/\mathrm{d}x$), and the constants 0.5 and 1 are selected such that $\int_0^1 \theta(k)\mathrm{d}k = 1$. Thus, $\int \theta(k)\mathrm{d}k = 0.5(mx^2 - mx) + x + C$ with $C = 0$, and then $\int_0^1 \int \theta(k)\mathrm{d}k\mathrm{d}k = (6x^2 - m[3x^2 - 2x^3])/12|_0^1 = (6 - m)/12$. To ensure that $\int_0^x \theta(k)\mathrm{d}k$ is positive in the whole transect, m is restricted to $[-2,2]$ and then Eqn 17 results in

$$c_w = c_i - r_{ias} A_s \frac{6 - m}{12} \quad \text{Eqn 18}$$

Finally, to estimate c_w from adaxial and abaxial measurements with a known R_{ias}, assuming that Θ_{ad} and Θ_{ab} have the same m value, we obtain (see full derivation in Supporting Information Notes S1)

$$c_w = \frac{c_{i-ad} A_{s-ab} + c_{i-ab} A_{s-ad} - \Theta R_{ias} A_{s-ad} A_{s-ab}}{A_{s-T}} \quad \text{Eqn 19}$$
$$c_w = \frac{c_{i-ad} A_{s-ab} + c_{i-ab} A_{s-ad} - \frac{(6 - m) R_{ias} A_{s-ad} A_{s-ab}}{12}}{A_{s-T}}$$

We have included a simple R script for the calculations in Notes S2.

Note that in the special case of assuming homogeneous photosynthetic uptake in the transect, $\theta(x) = 1$ or $m = 0$, that is, linear cumulative photosynthetic uptake in the transect, we obtain $A_s/2 = (c_i - c_w)/r_{ias}$, which is equivalent to the equation presented by Parkhurst *et al.* (1988) and identical to that used by Wong *et al.* (2022) based on assimilation rate per unit mesophyll volume if $c_w = c_{i\text{-}ab}$, an assumption specific to the particular experimental setup in that study.

Materials and Methods

Calculation of c_i

The impact on c_i calculations of neglecting cuticular fluxes using von Caemmerer & Farquhar (1981) equations has been discussed in previous studies (Boyer *et al.*, 1997; Boyer, 2015; Hanson *et al.*, 2016; Lamour *et al.*, 2021; Márquez *et al.*, 2021a,b). Márquez *et al.* (2021a) equations (MSF) include the cuticular conductance from the outset of the derivation, so MSF equations are used for the main analyses here. A brief recapitulation of the analyses including von Caemmerer and Farquhar calculations is included in Notes S3.

Plant material

Seventeen plants were used during our experiments: five *Capsicum annuum* L., six *Helianthus annuus* L., and six *Gossypium hirsutum* L., and data were collected from 11 *C. annuum*, 12 *H. annuus*, and 12 *G. hirsutum* leaves. Plants were grown from seeds in 3 l pots filled with Martins (*sic*) Potting Mix (Martins Fertilizers, Yass, NSW, Australia). Five grams of slow-release Osmocote Exact fertilizer (Scotts Australia, Bella Vista, NSW, Australia) was applied at the sowing time and another 5 g was applied 8 wk later. After sowing, all plants were kept in a glasshouse under natural light, with a temperature of 28°C during the day, 20°C at night, and watered once a day. The analyses were performed on fully expanded leaves.

The adaxial and abaxial cuticular conductances to water vapor (Table 2) were estimated using the Red-light technique introduced by Márquez *et al.* (2021b).

Measurements

Experiments were carried out on a gas exchange analysis system built by Wong *et al.* (1978, 1985a, 2022), which employs two LI-6251 gas analyzers (Li-Cor, Lincoln, NE, USA) to measure the CO_2 concentration of the upper and lower cuvettes independently. Additionally, two LI-6800 gas exchange analyzers (Li-

Table 2 Cuticular conductance to water (g_{cw}) for the leaves used in this study (average ± SD).

	g_{cw} (mmol m^{-2} s^{-1})		S_r	
Species	Adaxial	Abaxial	Value	Source
Capsicum annuum	5 ± 1.0	5.5 ± 0.8	0.13	Measured in this study
Helianthus annuus	5 ± 1.1	5 ± 1.0	0.83	Furukawa (1992); Nascimento *et al.* (2016)
Gossypium hirsutum	1.5 ± 0.4	1.5 ± 0.5	0.5	Lei *et al.* (2018)

S_r, stomatal density ration (adaxial over abaxial).

Cor) were used simultaneously to evaluate the gas exchange from the adaxial and abaxial surfaces of the leaf using the setup presented by Márquez *et al.* (2021a). The pressure in the upper and lower cuvettes was kept equal at 0.1 kPa above atmospheric.

The atmospheric conditions were set equal within each cuvette, that is, the same temperature, c_a and w_a, and thus the calculation of all the gas exchange parameters (i.e. g_{sw}, w_s, c_s, and c_i) could also be performed as if the measurements were taken in a single chamber, that is, mixing the adaxial and abaxial gases. Then, the gas exchange parameters were calculated using MSF equations for single surface gas exchange and mixed adaxial and abaxial gases. This permitted us to perform precise comparisons of single and double cuvette results as well as the estimation of c_w at different atmospheric and light conditions.

We define our standard conditions to emulate benign atmospheric conditions: 1 kPa of air saturation deficit (ASD), c_a of 400 μmol mol^{-1}, and light intensity of 1000 μmol m^{-2} s^{-1}. All the leaves were measured at standard conditions to evaluate the expected CO_2 gradients within the leaf of each species near natural conditions. Then, five leaves (two *G. hirsutum*, two *H. annuus* and one *C. annuum*) were selected to conduct experiments varying atmospheric and light conditions as describes below.

We applied different ASDs to the leaf to induce changes in stomatal conductance: measurements were taken on a *G. hirsutum* leaf under the nonstressful condition of 1 kPa ASD, mild stress of 1.5 kPa ASD, and moderate stress of 2 kPa. For the three conditions, the leaves were acclimatized for 30 min, with c_a set at 400 μmol mol^{-1}. An ASD response curve was performed for an *H. annuus* leaf, and readings were taken at ASDs of 1, 1.2, 1.5, 2, and 2.5 kPa when stomatal conductances of both sides of the leaf were stable (Table 3) for at least 10 min.

We applied different atmospheric CO_2 concentrations to the leaf to induce different CO_2 gradients between the atmosphere and the substomatal cavities: measurements were taken on a *C. annuum* leaf with the upper and lower chamber conditions set at 222, 425, and 859 μmol mol^{-1} and with stomatal conductance remaining stable for at least 15 min. Additionally, an A-c_i curve was performed on an *H. annuus* leaf, with air saturation deficit set to 1 kPa, light intensity at 1000 μmol m^{-2} s^{-1}, and readings were taken at c_a of 400, 300, 200, 100, 50, 100, 400, 600, 800, 1000, 1000, 1500, 2000, and 50 μmol mol^{-1} with a waiting period of 5 to 8 min between concentrations.

We applied different light intensities to induce different assimilation rates at high stomatal conductance and constant atmospheric CO_2 concentration: a *G. hirsutum* leaf was kept at 1 kPa of ASD and 400 μmol mol^{-1} of c_a and exposed to 1000, 1500, 800, 500, 100, and 10 μmol m^{-2} s^{-1} of light intensity, waiting 4 to 8 min between measurements.

Estimation of mesophyll air resistance to CO_2 diffusion

We followed the Wong *et al.*'s (2022) approach to estimating R_{ias}, which is to keep a constant CO_2 concentration in the upper cuvette at about atmospheric [CO_2] (400 μmol mol^{-1}) and reduce the CO_2 concentration in the lower cuvette until the assimilation of the lower surface reaches zero. Then, under these conditions, abaxial c_i equals c_w and Eqn 18 can be used to estimate R_{ias}, having chosen m (rate of change in photosynthetic uptake with x (du/dx)). In practice, the value of m is unknown and likely to be variable between leaves, so we approximate it as $m = -0.31$ (see Notes S4) based on the noble gas experiments of Wong *et al.* (2022). The impact of varying m in c_w estimations is discussed later.

The internal airspace resistance to CO_2 diffusion of each leaf was assessed, see Table S1 for the whole list, and find the R_{ias} values estimated for the leaves used for the variable environmental condition experiments in Table 4.

Table 3 Criteria to consider gas exchange readings as stable (when applicable).

Parameter	Units	Elapse (s)	Slope	SD
Stomatal conductance	mol m^{-2} s^{-1}	600	<0.001	<0.005
Assimilation rate	μmol m^{-2} s^{-1}	300	<0.05	<0.1
Transpiration rate	mol m^{-2} s^{-1}	300	<0.005	<0.00001

The instrument reads each second. Elapse represents the minimum time of readings to evaluate stability; Slope is the linear trend of the data during the lapse; and SD is the standard deviation of the readings during the lapse.

Table 4 Mesophyll air resistance to CO_2 (R_{ias}) of the leaf used in each experiment.

Species	Experiment	R_{ias} (m^2 s mol^{-1})
Capsicum annuum	c_a	7.5
Helianthus annuus	c_a	4.1
Helianthus annuus	ASD	4.1
Gossypium hirsutum	ASD	4
Gossypium hirsutum	Light intensity	4.5

Mesophyll conductance

The variable J method (Harley *et al.*, 1992) was used to estimate mesophyll conductance to CO_2 (g_m),

$$g_m = \frac{A}{c_x - \frac{\Gamma^*[J_a + 8(A+R_d)]}{J_a - 4(A+R_d)}} \quad \text{Eqn 20}$$

where A is assimilation rate, R_d is the respiration rate under the light conditions, Γ* is the CO_2 compensation point in the absence of R_d, J_a is the actual rate of photosynthetic electron transport and c_x is either $c_{i\text{-Mix}}$ or c_w. For the purpose of the comparison of calculations of g_m using $c_{i\text{-Mix}}$ or c_w the electron transport rate was used as a proxy of J_a, which is a rough approximation (Pons *et al.*, 2009), but close enough for the purposes of comparing results using different estimations of CO_2 concentration.

Calculation comparisons

We have compared the calculation of intercellular CO_2 concentrations using different approaches. To simplify the notation, we

have defined: the difference between adaxial and abaxial c_i estimates as Δc_i ($\Delta c_i = c_{i\text{-}ad} - c_{i\text{-}ab}$); the difference between the c_i estimated using the combined gas fluxes and the adaxial or abaxial fluxes as Δc_{Mix} ($\Delta c_{Mix} = c_{i\text{-}Mix} - c_{i\text{-}ad}$ or $\Delta c_{Mix} = c_{i\text{-}Mix} - c_{i\text{-}ab}$); the difference between the c_i estimated using the combined gas fluxes and c_w as Δc_{MW} ($\Delta c_{MW} = c_{i\text{-}Mix} - c_w$); and the difference between the c_w estimated using $m = -0.31$ and that with different m values in Eqn 19 as Δc_w ($\Delta c_w = c_w(-0.31) - c_w(m)$).

Results

Each species (see Table S1) presented different gradients between adaxial/abaxial c_i and c_w (Table 5), where the greatest gradient was found in the surfaces with higher stomatal density and conductance.

In general, we found that mixing adaxial and abaxial fluxes leads to an averaged result of both c_i values weighted by the assimilation rate (A). The detailed results of the experiments described in 'Measurements' in the Materials and Methods section are presented below.

Different atmospheric [CO_2]

Different total assimilation rates were achieved by varying c_a around *C. annuum* and *H. annuus* leaves (Fig. 2a,d). The partitioning of A between adaxial and abaxial surfaces was stable in the *C. annuum* leaf, where the abaxial surface was the main driver for the changes and the adaxial surface assimilation rate remained relatively constant. In the case of the *H. annuus* leaf, A of both surfaces varied with each c_a. A increased with c_a as the latter varied from 50 to 500 μmol mol^{-1}. However, with further increases in c_a, the abaxial surfaces increased A while the adaxial surfaces decreased it, without a significant change in the total assimilation rate. Δc_i values in *C. annuum* were between 10 and 40 μmol mol^{-1} under the imposed c_a, and in *H. annuus* Δc_i values were between 2 and 7 μmol mol^{-1}. Δc_{Mix} estimates were between −5 and 25 μmol mol^{-1} in *C. annuum*, and between −2 and 5 μmol mol^{-1} in *H. annuus*.

As expected, the estimated c_w values were below the adaxial and abaxial c_i; and Δc_{MW} was always positive. In *C. annuum*, the c_w tended to be near the adaxial c_i as the assimilation rate of the adaxial surfaces was near 0; the differences between adaxial and abaxial c_i and c_w in *H. annuus* were from < 1 μmol mol^{-1} at low c_a up to *c.* 15 μmol mol^{-1} at high c_a.

Table 5 Average CO_2 drawdown within the leaf (average ± SD) measured at conditions of air saturation deficit (ASD) = 1 kPa, c_a = 400 μmol mol^{-1}, and light intensity of 1000 μmol m^{-2} s^{-1}.

	No. of leaves	$c_{i\text{-}ad} - c_w$ (μmol mol^{-1})	$c_{i\text{-}ab} - c_w$ (μmol mol^{-1})
Capsicum annuum	10	4.0 ± 0.7 a	10.0 ± 1.2 b
Helianthus annuus	10	15.0 ± 4.8 a	16.9 ± 3.0 a
Gossypium hirsutum	10	12.4 ± 3.3 a	18.8 ± 3.7 b

Distinct letters in the same row indicate statistical differences with a *P*-value < 0.001 using the Student's *t*-test and Tukey at 95% confidence. c_i is the CO_2 concentration in the substomatal cavity, c_w is the CO_2 concentration at the surface of mesophyll cells, ad and ab subscripts stand for adaxial and abaxial, respectively.

Different air saturation deficits

Application of three air moisture saturation deficits (ASD) to a *G. hirsutum* leaf resulted in Δc_i from 5 to 27 μmol mol^{-1} when ASD varied from 1 to 2 kPa (Fig. 3). The *G. hirsutum* leaf presented a fairly constant stomatal conductance to water vapor (g_{sw}) from the upper surface of *c.* 0.06 mol m^{-2} s^{-1} whilst the lower surface g_{sw} showed more variation from 0.25 to 0.2 mol m^{-2} s^{-1} at 1 kPa and 2 kPa of ASD, respectively. In an *H. annuus*, leaf nonzero Δc_i was evident only under ASD equal to, or >1.5 kPa (Fig. 3); Δc_i was as large as almost 50 μmol mol^{-1} under the highest ASD.

In both species, the calculated $c_{i\text{-}Mix}$ remained between the values estimated separately for each side of the leaf. Δc_{Mix} became larger as the ASD increased (Fig. 3c,f), presenting a Δc_{Mix} of *c.* 20 μmol mol^{-1} in *G. hirsutum*, and as large as almost −30 μmol mol^{-1} in *H. annuus*.

The estimate of c_w in *G. hirsutum* was always lower than the estimated adaxial and abaxial c_i, but the difference was reduced as the ASD increased; similar observations were made in *H. annuus* but at ASD above 1.5 kPa, the estimated c_w fell between the adaxial and abaxial c_i, which is impossible. These two unusual observations might be an indication of unsaturation occurring in the mesophyll airspace of the leaf, as described by Wong *et al.* (2022), or patchy stomatal conductance (Mott & Buckley, 2000): these issues will be addressed in more detail in the discussion.

Different light intensities

A light response curve from a *G. hirsutum* leaf showed that Δc_{Mix} was below 5 μmol mol^{-1} in most cases (Fig. 4). The adaxial and abaxial stomatal conductances did not change greatly during the experiment, being *c.* 0.05 and 0.225 mol m^{-2} s^{-1}, respectively. We found that the larger Δc_{Mix} occurred with measurements near the light compensation point.

As expected, the estimated c_w was below the estimated adaxial and abaxial c_i, except at the lowest light intensity where the assimilation of the adaxial surfaces was almost zero and the assimilation of the abaxial surfaces was negative. Note that at the lowest light intensity in our experiment, c_w was expected to be near the adaxial c_i but higher than the abaxial c_i to allow CO_2 to move from the inside of the leaf to the lower cuvette.

Adaxial and abaxial ratios

The values obtained for $g_{sw\text{-}ad} : g_{sw\text{-}ab}$, $c_{i\text{-}ad} : c_{i\text{-}ab}$, $c_{s\text{-}ad} : c_{s\text{-}ab}$, and $w_{s\text{-}ad} : w_{s\text{-}ab}$ were variable between species and among different environmental conditions (Table 6). Adaxial and abaxial values of g_{sw}, c_i, c_s, and w_s were never identical, impacting the $c_{i\text{-}Mix}$ estimation to different degrees with no clear predictable patterns. This confirms our hypothesis that it is incorrect to assume that

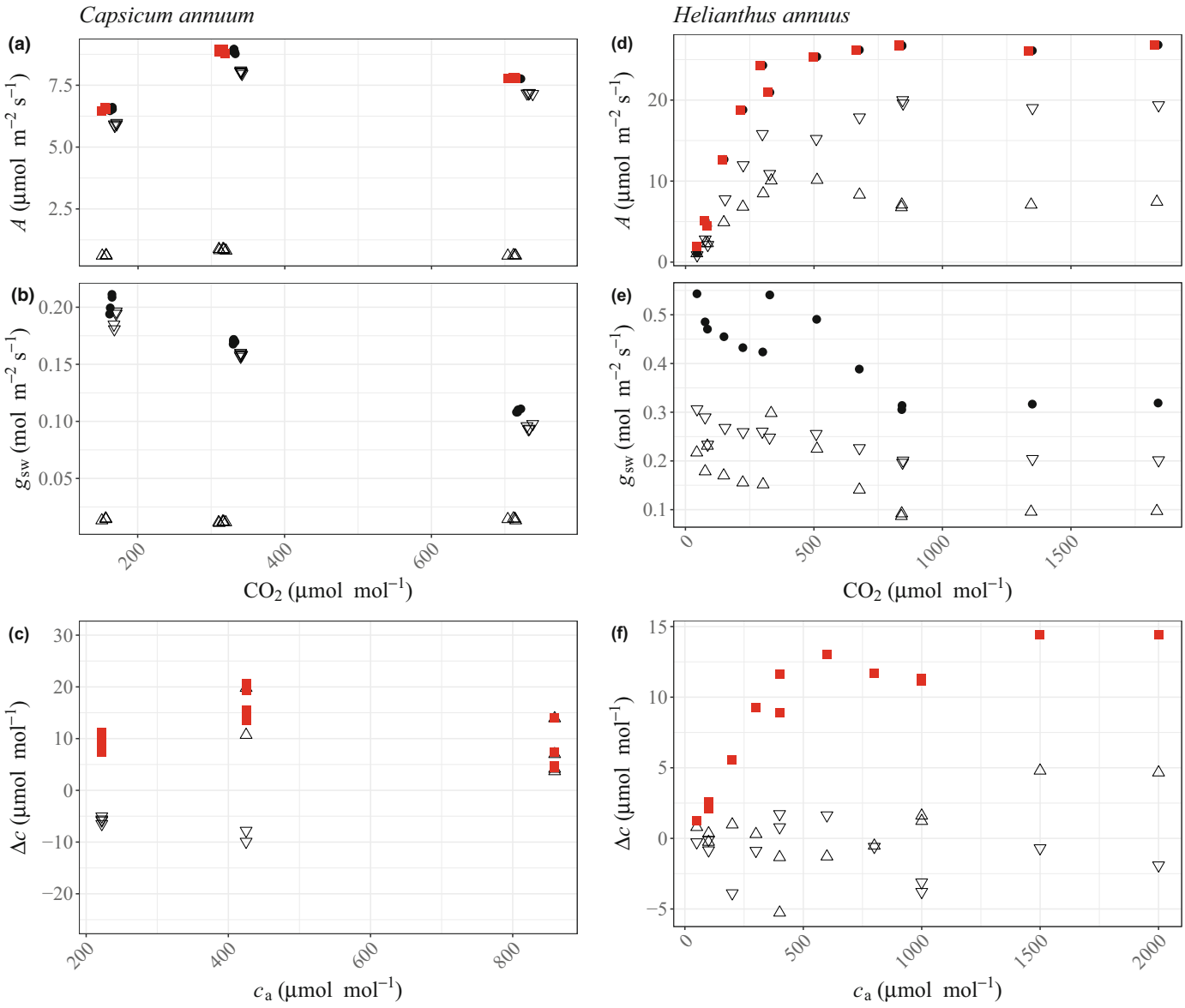

Fig. 2 Responses of *Capsicum annuum* (a–c) and *Helianthus annuus* (d–f) leaves to varying the atmospheric CO_2 concentration (c_a). In (a, b, d, e), data from the abaxial surface are the inverted triangles (▽); adaxial surfaces the triangles (△); mix of gases are the black dots (●) and values using c_w are the red squares (■). (a, d) assimilation vs calculated internal CO_2 concentration using gas exchange fluxes from the abaxial surfaces, adaxial surfaces, the combination of fluxes and the estimated c_w; (b, e) adaxial, abaxial and total stomatal conductance; and (c, f) the difference between the [CO_2] estimated from the combination of gases and each surface of the leaf ($\Delta c_{Mix} = c_{i\text{-}Mix} - c_{i\text{-}ad}$ (△); $\Delta c_{Mix} = c_{i\text{-}Mix} - c_{i\text{-}ab}$ (▽); and $\Delta c_{MW} = c_{i\text{-}Mix} - c_w$ (■)).

the differences between adaxial and abaxial values are negligible and proves that significant variations can be found even if the atmospheric conditions of upper and lower cuvettes are the same.

We found that the variability in $g_{sw\text{-}ad} : g_{sw\text{-}ab}$, $c_{i\text{-}ad} : c_{i\text{-}ab}$, $c_{s\text{-}ad} : c_{s\text{-}ab}$, and $w_{s\text{-}ad} : w_{s\text{-}ab}$ became even more challenging if we were to predict under non-steady-state conditions such as when stomatal conductance increases during light induction (Notes S5).

Effect of *m* in c_w calculations

Even though varying the rate of change of photosynthetic uptake with $x(m)$ impacts the estimation of R_{ias} (see Notes S4), it does not significantly affect the estimation of c_w, having an impact of a fraction of a μmol mol^{-1} variability at most (Fig. 5). The $\Delta c_w = c_w(-0.31) - c_w(m)$ shown in Fig. 5 were calculated using the same m in the calculation of R_{ias} and c_w but we observe that variations of m within ±1 in the calculation of R_{ias} and c_w did not significantly affect the c_w estimation either (data not shown).

Discussion

Adaxial and abaxial gas exchange and the mix of gases

It can be seen from the measurements of internal resistance to CO_2 diffusion that the species used in this study do not present significant physical impediments to diffusion within the intercellular airspace, though they do have different stomatal density ratios (see Table 2). Thus, Δc_{Mix} ($\Delta c_{Mix} = c_{i\text{-}Mix} - c_{i\text{-}ad}$ or

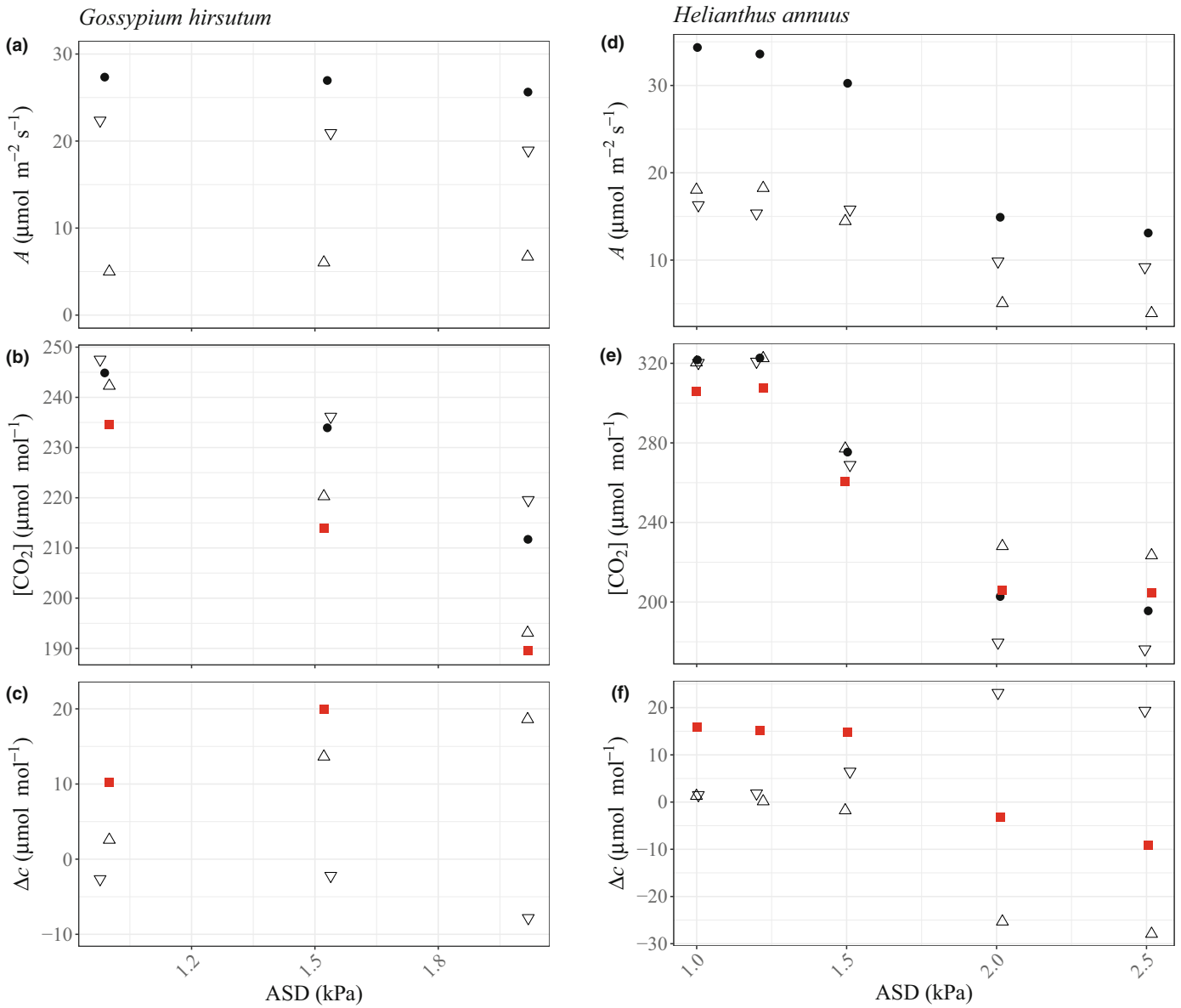

Fig. 3 Responses of *Gossypium hirsutum* (a–c) and *Helianthus annuus* (d–f) leaves to varying the air saturation deficit (ASD). In (a, b, d, e), data from the abaxial surface are the inverted triangles (▽); adaxial surfaces the triangles (△); mix of gases are the black dots (●), and values using c_w are the red squares (■). (a, b) assimilation rate vs ASD; (b, e) calculated leaf internal CO_2 concentration using gas exchange fluxes from the abaxial surfaces ($c_{i\text{-}ab}$, inverted triangles), adaxial surfaces ($c_{i\text{-}ad}$, triangles), the combination of fluxes ($c_{i\text{-}Mix}$, black dots), and the estimated c_w (red squares) vs ASD; and (c, f) the difference between the substomatal $[CO_2]$ estimated from the combination of gases and each surface of the leaf ($\Delta c_{Mix} = c_{i\text{-}Mix} - c_{i\text{-}ad}$ (△); $\Delta c_{Mix} = c_{i\text{-}Mix} - c_{i\text{-}ab}$ (▽); and $\Delta c_{MW} = c_{i\text{-}Mix} - c_w$ (■)).

$\Delta c_{Mix} = c_{i\text{-}Mix} - c_{i\text{-}ab}$) can be attributed mostly to different resistances to CO_2 diffusion between the adaxial and abaxial surfaces. During our experiments, ASD below 1.2 kPa and c_a equal to or below 400 μmol mol^{-1} gave Δc_{Mix} below 5 μmol mol^{-1} in *H. annuus*; but for *G. hirsutum* only at low light intensities was $\Delta c_{Mix} > 5$ μmol mol^{-1} and for *C. annuum* under all the conditions Δc_{Mix} was > 5 μmol mol^{-1}. These results indicate that leaf features such as the stomatal density ratio affect the reliability of the $c_{i\text{-}Mix}$ estimation unpredictably. This highlights the risk of error from combining the adaxial and abaxial fluxes as mixing the fluxes hides differences resulting from the physical structure of the leaf, especially in plants under stress.

In amphistomatous leaves, when stomata are open and under no stress, it has been shown that the ratio $c_{i\text{-}ad} : c_{i\text{-}ab}$ is close to one (Mott & O'Leary, 1984; Wong *et al.*, 1985b,c; Parkhurst *et al.*, 1988). However, $c_{i\text{-}ad} : c_{i\text{-}ab}$ diverges from one in leaves that present internal leaf structures affecting gas diffusion between adaxial and abaxial stomatal cavities (Farquhar & Raschke, 1978; Long *et al.*, 1989) and, as was shown here, when the stomatal density ratio (adaxial : abaxial) is substantially different from one (see *C. annuum*).

After mixing the gases, we must adjust the calculations accordingly to account for the differences between the adaxial and abaxial surfaces. For instance, to estimate g_{sw}, c_i, w_s, and c_s, we can

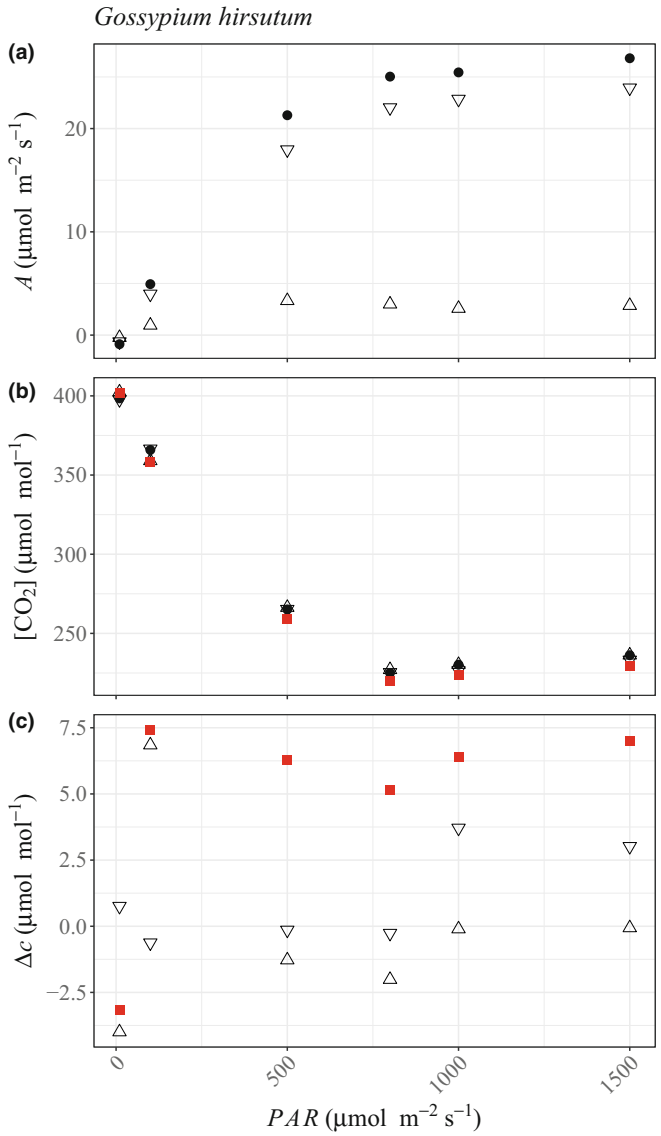

Fig. 4 *Gossypium hirsutum* leaf responses whilst varying the photosynthetically active radiation (PAR). (a) Assimilation light response; (b) CO_2 concentration within the leaf, c_i estimated using the gas exchange fluxes from the abaxial surfaces (▽), adaxial surfaces (△), the combination of fluxes (●) and the estimated c_w (■); and (c) the difference between the $[CO_2]$ estimated from the combination of gases and each surface of the leaf ($\Delta c_{Mix} = c_{i\text{-}Mix} - c_{i\text{-}ad}$ (△); $\Delta c_{Mix} = c_{i\text{-}Mix} - c_{i\text{-}ab}$ (▽); and $\Delta c_{MW} = c_{i\text{-}Mix} - c_w$ (■)).

incorporate a variable that relates adaxial and abaxial characteristics, such as $g_{sw\text{-}ad} : g_{sw\text{-}ab}$, and $c_{i\text{-}ad} : c_{i\text{-}ab}$ (see Notes S6). Equations in Notes S6 are a more accurate approach than assuming a single internal $[CO_2]$ at one virtual substomatal cavity when adaxial and abaxial fluxes are mixed. However, even when a leaf has a known cuticular conductance, to calculate g_{sw}, the value $g_{sw\text{-}ad} : g_{sw\text{-}ab}$ remains unknown after the mixing, and in practice, the only known value to calculate c_i using Notes S6 equations is the total assimilation rate.

The differences between adaxial and abaxial stomatal behavior vary among species and with conditions, making it difficult to isolate a set of parameters that would allow us to predict the

Table 6 Mixing ratios obtained from the experiments; bold values are those found at benign ambient conditions ($c_a \approx 400$ μmol mol^{-1}, PAR = 1000 μmol m^{-2} s^{-1} and ASD ≈ 1 kPa).

Plant	Experiment	$g_{sw\text{-}ad} : g_{sw\text{-}ab}$	$c_{i\text{-}ad} : c_{i\text{-}ab}$	$c_{s\text{-}ad} : c_{s\text{-}ab}$	$w_{s\text{-}ad} : w_{s\text{-}ab}$
Gossypium hirsutum	ASD: **1**; 1.5; 2 kPa	**0.22**; 0.27; 0.36	0.98; 0.97; 0.96	**1.01**; 1.01; 1.01	**0.97**; 1.00; 0.94
Helianthus annuus	ASD: **1**, 1.2; 1.5; 2; 2.5 kPa	**1.11**; 1.22; 0.97; 0.66; 0.54	**1.00**; 1.01; 1.03; 1.27; 1.27	**1.00**; 1.00; 1.00; 1.01; 1.01	**1.00**; 0.99; 1.00; 0.98; 0.95
Capsicum annuum	c_a: 222; **425**; 859 μmol mol^{-1}	0.08; **0.08**; 0.07	0.92; **0.93**; 0.95	1.01; **1.01**; 1.01	0.93; **0.92**; 0.96
Helianthus annuus	c_a: **400**; 300; 200; 100; 50; 100;	**0.58**; 0.60; 0.64; 0.62; 0.71;	**1.01**; 0.99; 0.97; 1.00; 0.98;	**1.01**; 1.01; 1.01; 1.00; 0.99;	**1.00**; 1.00; 1.00; 1.01; 1.00;
	400; 600; 800; 1000; 1000; 1500;	0.99; **1.20**; 0.88; 0.62; 0.44;	0.99; **1.02**; 1.01; 1.00; 0.99;	0.99; **1.00**; 1.01; 1.01;	1.01; **1.00**; 1.00; 1.00; 1.00;
	2000 μmol mol^{-1}	0.46; 0.47; 0.48	0.99; 1.00; 1.00	1.01; 1.01; 1.01; 1.00	1.00; 1.00; 1.00
Gossypium hirsutum	PAR: **1000**; 1500; 800; 500; 100;	**0.11**; 0.12; 0.13; 0.18;	**1.00**; 1.01; 1.01; 1.00;	**1.01**; 1.01; 1.01; 1.01; 1.00;	**1.01**; 1.00; 0.98; 0.98; 1.01; 1.02
	10 μmol m^{-2} s^{-1}	0.18; 0.19	0.98; 1.01	1.00	

Ratio of adaxial over abaxial stomatal conductance ($g_{sw\text{-}ad} : g_{sw\text{-}ab}$), substomatal cavity CO_2 concentration ($c_{i\text{-}ad} : c_{i\text{-}ab}$), CO_2 concentration at the surfaces of the leaf ($c_{s\text{-}ad} : c_{s\text{-}ab}$), and water vapor concentration at the surface of the leaf ($w_{s\text{-}ad} : w_{s\text{-}ab}$). Experimental conditions varying the air saturation deficit (ASD), atmospheric CO_2 concentration (c_a), and photosynthetically active radiation (PAR).

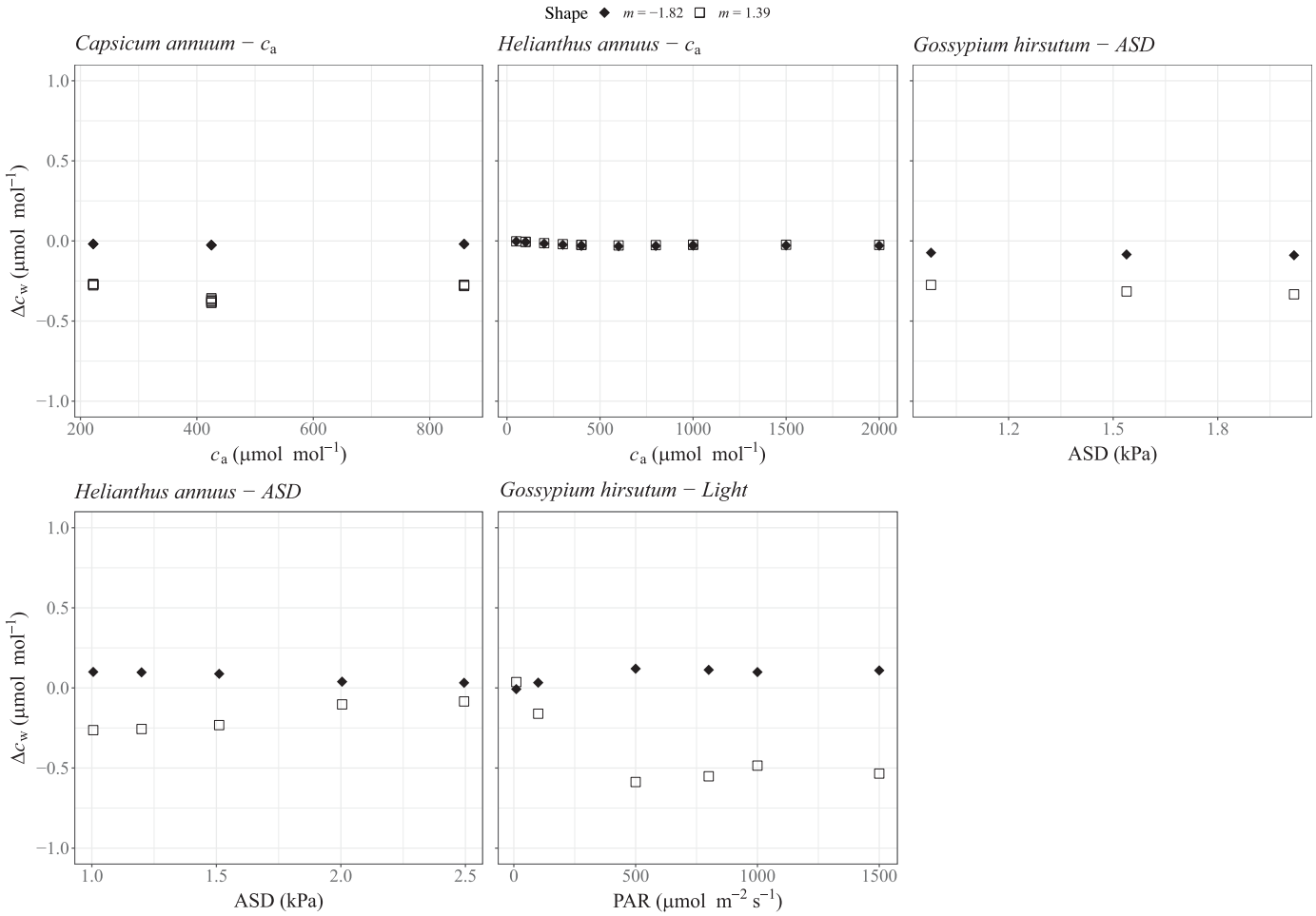

Fig. 5 Variability of c_w using different $m = -1.82$ and 1.39 in Eqn 19. Data from Figs 1–3. $\Delta c_w = c_w(-0.31) - c_w(m)$. Δc_w for the experiments varying the atmospheric CO_2 concentration (c_a), the air saturation deficit (ASD), and the photosynthetically active radiation (PAR).

behavior of $g_{sw\text{-}ad} : g_{sw\text{-}ab}$, $c_{i\text{-}ad} : c_{i\text{-}ab}$, $c_{s\text{-}ad} : c_{s\text{-}ab}$, and $w_{s\text{-}ad} : w_{s\text{-}ab}$. As the stomatal density ratio (adaxial over abaxial) has an important impact on the fluxes, a tentative option is to use it to predict $g_{sw\text{-}ad} : g_{sw\text{-}ab}$ to separate adaxial and abaxial transpiration (E). To do so, we must assume vapor saturation within the leaf and identical adaxial and abaxial boundary layers, allowing us to estimate w_s and g_{sw} for each surface. Nevertheless, even in conditions where the gradient w_i–w_a is the same for both surfaces, the stomatal density ratio is not a good approximation of the stomatal evaporation ratio and $g_{sw\text{-}ad} : g_{sw\text{-}ab}$ (Anderson & Briske, 1990). Thus, this approach would need to account for the stomatal aperture ratio (adaxial over abaxial), which is known to be variable, for example, between 0.75 and 0.9 (Aston, 1978; Pemadasa, 1979; Pearson *et al.*, 1995; Wang *et al.*, 1998) and as we observed here, is not constant for a single leaf under different conditions. Furthermore, the stomata can differ in depth even at a known stomatal aperture ratio and stomatal density ratio. For the estimation of c_s and $c_{i\text{-}ad} : c_{i\text{-}ab}$, we have the same issues described above in addition to the unknown CO_2 concentration in the internal leaf airspace.

In some cases, part of the impact of abaxial and adaxial fluxes is incorporated at the time of calculating stomatal conductance to H_2O, using a correction factor that relates the abaxial and adaxial stomatal conductances ($K = g_{sw\text{-}ab}/g_{sw\text{-}ad}$) (Li-Cor, 2020). This correction factor is used to account for the impact of differences in adaxial and abaxial stomatal conductance, and the boundary layer conductance (g_{bw}) of each surface on the total conductance to water. However, K does not include the impact of the actual partition of fluxes on the adaxial and abaxial surfaces and requires previous knowledge of the adaxial and abaxial g_{sw}. Yet, in most cases, K has a minor impact on the calculations because g_{bw} is large within the chamber and assumed identical for each surface.

This means that using leaf features as a guide to artificially splitting adaxial and abaxial fluxes after a combined measurement makes it challenging to obtain more reliable results than those from previous assumptions when adaxial and abaxial fluxes were mixed. Thus independent gas exchange measurements of the adaxial and abaxial surfaces must be preferred.

Two sides, one CO_2 concentration c_w

As expected from our theory, c_w was *c.* 10 μmol mol^{-1} lower than the adaxial and abaxial c_i when estimated at about ambient atmospheric c_a (*c.* 400 μmol mol^{-1}) (see Table 5). Assessing the

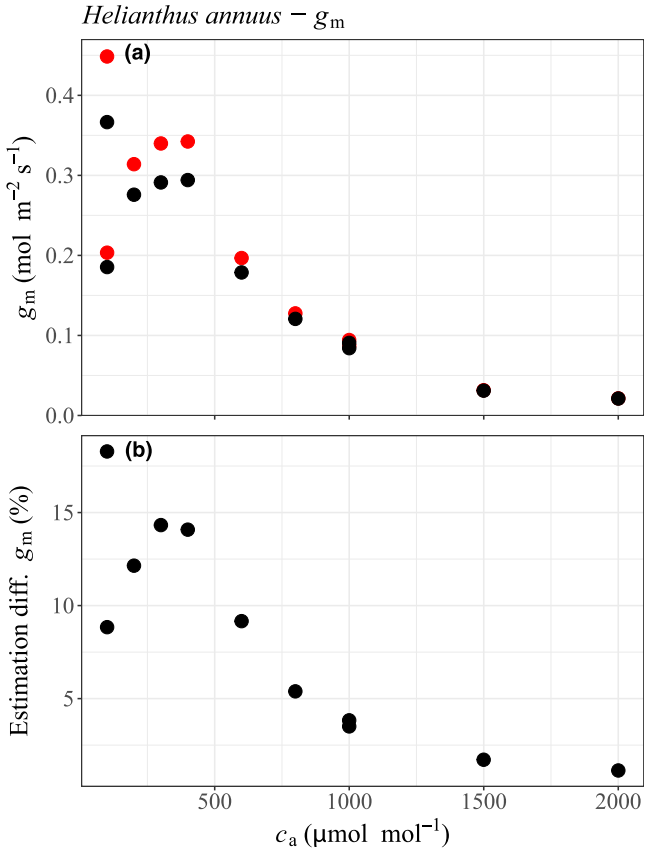

Fig. 6 Estimation of mesophyll conductance to CO_2 (g_m) from data in Fig. 2. (a) Calculations of g_m using c_w (red) and $c_{i\text{-}Mix}$ (black). (b) Difference between g_m estimated using c_w and $c_{i\text{-}Mix}$ (Diff.g_m = 100[$g_m(c_w)$ − $g_m(c_{i-Mix})$]/$g_m(c_w)$).

gas exchange of each surface independently allows us to explore physiological responses accounting for the behavior of each side, but also brings us to the practical issue of ending up with two different c_i values, which might be a problem for some common calculations. The impact of including c_w on the calculation varies; for instance, we found in our experiments a minor effect in the estimation of biochemical parameters but a larger effect in the estimation of mesophyll conductance to CO_2. See both examples below.

A-c_i curves are usually fitted to the data using the Farquhar *et al.* (1980) model, obtaining the biochemical parameters of maximum carboxylation rate (V_{cmax}), the maximum rate of carboxylation allowed by the potential electron transport (J_a) at a particular light intensity and temperature, triose phosphate utilization (TPU), and dark respiration (R_d). In the *A*-c_i curve presented in Fig. 2d, we found two estimated values for c_i: adaxial and abaxial. Thus, the fitting can give us two possible outcomes for each parameter. Assuming infinite mesophyll conductance, we obtain (ad & ab): V_{cmax} = 102.8 and 97.5; J = 129.3 and 128.3; TPU = 9.3 and 9.2; and R_d = 1.6 and 1.4 µmol m^{-2} s^{-1}. The introduction of c_w instead of c_i into the calculation of the biochemical parameters gives a single value for each of them: V_{cmax} = 104.2; J = 129.5; TPU = 9.3; and R_d = 1.4 µmol m^{-2} s^{-1}. Thus, the differences in the estimation of biochemical parameters were small, but in some cases, these levels of uncertainty might not permit the most demanding interpretation of different biological trends.

The inclusion of c_w facilitates mesophyll conductance (g_m) estimations by accounting for R_{ias}. In a rough calculation using the variable J method to estimate g_m (Harley *et al.*, 1992), equating J to ETR obtained with fluorescence measurements, we can see that the g_m values estimated using c_w differ from those estimated using $c_{i\text{-}Mix}$ (Fig. 6a). At atmospheric c_a (400 µmol mol^{-1}), we found that the g_m estimated from $c_{i\text{-}Mix}$ was *c.* 15% lower than the g_m estimated using c_w. Estimations using c_w were higher than those using $c_{i\text{-}Mix}$ in all the measurements, ranging from 18% to 1% difference in the estimates (Fig. 6b). The inclusion of c_w gives a more detailed description of the CO_2 gradients within the leaf and a better interpretation of the gaseous and liquid paths of CO_2 diffusion.

High air saturation deficit measurements

Extra care must be taken with water-stressed leaves, as estimations of gas exchange are based on the assumption of w_i being at saturated conditions ($w_i = w_{sat}$) and that the whole surface of the leaf contributes to the exchange. However, it has been shown that under high ASD, patchiness (Mott & Buckley, 2000), or unsaturation may occur (Cernusak *et al.*, 2018), and the mixture of adaxial and abaxial fluxes might mask the occurrence of both. The failure of one or both of these assumptions compromizes the validity of the results, making their identification crucial (Rockwell *et al.*, 2022). The measurements presented in Fig. 3 for *G. hirsutum* and *H. annuus* both exhibit oddities. *Gossypium hirsutum* presented considerably different c_w at different ASD without significant changes in total assimilation rate and a reduction in the difference between adaxial c_i and c_w while ASD increased without a significant reduction in adaxial assimilation. *Helianthus annuus* estimation of c_w presented values between the adaxial and abaxial c_i while the ASD increased, which is impossible as c_w would have opposite gradients with each c_i. These two oddities are likely to be caused by unsaturation or patchiness and the principles presented by Wong *et al.* (2022) may help to identify when either of them occurs.

Wong *et al.* (2022) estimated unsaturation by cancelling out the assimilation rate on one surface of the leaf and assuming constant R_{ias}, and that the photosynthetic capacity is not affected by the increase of vapor pressure difference (VPD). They then used iteration to find a w_i that satisfies the expected adaxial-abaxial c_i difference at different ASD. We can generalize these principles using Eqn 19 to derive an equation for w_i (Eqn S7.6 in Notes S7), and then use data from a [CO_2] response curve at low VPD to estimate the target c_w for a given total assimilation rate. Using this approach, we found that the data of *G. hirsutum* in Fig. 3 presented a value of c_w lower than the one expected from the relation A/c_w measured under low ASD. Then, modifying the expected c_w in order to match the A/c_w measured under low VPD it appeared that $w_i < w_{sat}$ (Fig. 7). We found that using the same approach but with a normal A/c_i does not provide consistent results, even though sometimes it seems like a reasonable proxy

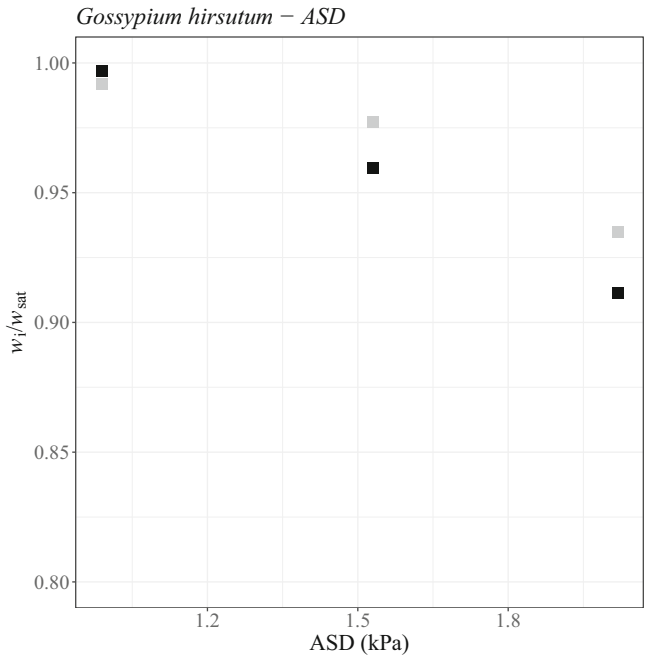

Fig. 7 Estimation of unsaturation from data in Fig. 3 using A-c_w (black) and A-c_i (grey) curves. ASD, air saturation deficit.

to detect unsaturation. On the contrary, *H. annuus* in Fig. 3 presented a value of A lower than the one expected from the A/c_w measured under low VPD, which is consistent with a leaf experiencing patchiness. Note that the correction in w_i using the equation presented in Notes S7 for *H. annuus* in Fig. 3 to match the relation A/c_w measured under low VPD would be $w_i > w_{sat}$, which is not possible because moisture would condense.

The calculations to estimate unsaturation shown in Fig. 7 are given in Notes S8 but more research is needed to evaluate and validate them under a broader range of conditions and for more species. Our future research will focus on the occurrence of unsaturation and patchiness, and how to account for it using the equations in this paper. The methods presented here may help improve the information extracted from gas exchange data, including the occurrence of unsaturation under any experimental setup that can measure adaxial and abaxial surfaces independently. Unfortunately, independent adaxial and abaxial measurement has not been a common practice recently and most devices do not include this feature. A possible alternative is to use the modification of two commercial LI-6800 devices presented by Márquez *et al.* (2021a) that allows measurements of both surfaces of the leaf simultaneously, as in this study.

Model insights

We presented Eqn 19 to estimate c_w accounting for A_s and R_{ias}, which is a bounded equation for $\int \upsilon(k)\mathrm{d}k$ and $\rho(l)$ from our general derivation Eqn 10. The measured R_{ias} includes the effect of the tortuosity in the mesophyll gaseous path (τ) due to structures within the leaf such that $r = r(l, \rho(\tau))$ and $\tau = \tau(l)$. Equivalently, A_s comprizes the effect of light intensity, light capturing efficiency and the biochemical activity in the photosynthetic tissue in the mesophyll such that $u = u(l, \upsilon(I, b))$, $I = I(l)$ and $b = b(l)$. Thus, $\rho(l)$ and $\upsilon(l)$ are complex to determine independently; however, we took advantage of the fact that their evaluations from 0 to L are known. Interestingly, the estimation of c_w showed stability even when the shape of $\int \upsilon(k)\mathrm{d}k$ was varied significantly. This is due to the structure of Eqn 19, which is searching for a value that satisfies the gradient of CO_2 between surfaces accounting for a known total resistance (R_{ias}), and which in practice encompasses a narrow range of values, as can be seen in Fig. 5. The impact of $r(l)$ on c_w calculations was not directly tested but the test performed in $\Theta(l)$ varying m (Fig. 5) suggests that it should be minor. In general, the variation of $\upsilon(l)$ is expected to be larger than that of $\rho(l)$ with progress along the path, L.

In practice, Eqns 10 or 16 could be used to estimate any [CO_2] in the transect from the stomatal cavity to c_w; however, for those calculations, the bounds for $\int \upsilon(k)\mathrm{d}k$ and $\rho(l)$ are likely to be less flexible than those used for estimating c_w. For instance, the shape of the cumulative photosynthetic uptake ($\int \upsilon(k)\mathrm{d}k$) plays a major role in the estimations of concentrations in the transect other than c_w, as can be deduced from Notes S4. A similar argument applies for the assumption of constant $\rho(l)$, constant resistance to CO_2 diffusion per unit of length, where the shape of $\rho(l)$ may play a more significant role in calculating a c_l other than c_w.

Finally, our model uses c_i as input, and thus it carries the assumptions used to estimate the leaf surface resistance, to calculate c_i from gas exchange measurements. The use of models for estimating c_i such as von Caemmerer & Farquhar (1981) and Márquez *et al.* (2021a), usually assume that the CO_2 concentrations in the substomatal cavities are similar, that the stomatal cavity is at saturated conditions at leaf temperature and that the whole leaf surface is involved in the exchange (no patchiness). Regarding the latter two assumptions, in 'High air saturation deficit measurements' in the Discussion section, we have presented a method that can be used to evaluate the validity of these assumptions in the measurements and how to differentiate them.

Conclusion

The use of a device that includes measurements of the gas exchange independently on each side of the leaf allowed us to account for the mesophyll airspace resistances in the calculations of CO_2 concentrations within the leaf, permitting estimation of the CO_2 concentration at the surface of photosynthetic mesophyll cells (c_w). Accounting for c_w improves the information that can be extracted from gas exchange experiments, allowing us to provide a more detailed description of the CO_2 and vapor gradients within the leaf.

The miscalculations arising from the mixing of adaxial and abaxial fluxes are usually overlooked, especially when the measurements are made on plants with high stomatal conductance or under stable conditions. However, we have shown that these errors are variable, and even mild stresses or changes in CO_2 concentration might significantly impact the c_i calculation regardless of the stable gas exchange conditions. We showed that it is an incorrect generalization that there is a negligible difference between adaxial and abaxial

stomatal cavity CO_2 concentration when the adaxial and abaxial atmospheric conditions (c_a and w_a) are identical. Parity of c_i between the two sides only occurs in some cases and seems to depend on leaf structure. Mixing of gases from the upper and lower cuvette is a source of error in c_i calculations commonly found in leaf gas exchange measurements and the correction of this error after mixing is not feasible. Thus, the mix of adaxial and abaxial fluxes should be avoided in experiments that require high reliability of internal leaf [CO_2] estimations.

Acknowledgements

The authors would like to thank ANID, Doctorado Becas Chile/2015 Folio: 72160160, the ARC Centre of Excellence for Translational Photosynthesis and the ARC for DP210103186 for funding the research; Suan Chin Wong for providing technical support; ANU Plant Services for taking care of the plant material. Open access publishing facilitated by Australian National University, as part of the Wiley - Australian National University agreement via the Council of Australian University Librarians.

Competing interests

None declared.

Author contributions

DAM, HS-W, LAC, and GDF conceived the study. DAM designed the experiments. DAM undertook the experimental work and data analysis. DAM and GDF developed the theory and modeling. All authors contributed to concept development. DAM wrote the manuscript with help from all authors.

ORCID

Lucas A. Cernusak https://orcid.org/0000-0002-7575-5526
Graham D. Farquhar https://orcid.org/0000-0002-7065-1971
Diego A. Márquez https://orcid.org/0000-0002-5191-676X
Hilary Stuart-Williams https://orcid.org/0000-0002-9272-9178

Data availability

All generated and analyzed data from this study are included in the published article and its Supporting Information. Correspondence and requests for materials should be addressed to GDF.

References

Anderson VJ, Briske DD. 1990. Stomatal distribution, density and conductance of three perennial grasses native to the southern true prairie of Texas. *The American Midland Naturalist* **123**: 152–159.

Aston M. 1978. Differences in the behaviour of adaxial and abaxial stomata of amphistomatous sunflower leaves: inherent or environmental? *Functional Plant Biology* **5**: 211–218.

Boyer JS. 2015. Impact of cuticle on calculations of the CO_2 concentration inside leaves. *Planta* **242**: 1405–1412.

Boyer JS, Wong SC, Farquhar GD. 1997. CO_2 and water vapor exchange across leaf cuticle (Epidermis) at various water potentials. *Plant Physiology* **114**: 185–191.

Busch FA, Holloway-Phillips M, Stuart-Williams H, Farquhar GD. 2020. Revisiting carbon isotope discrimination in C_3 plants shows respiration rules when photosynthesis is low. *Nature Plants* **6**: 245–258.

von Caemmerer S, Farquhar GD. 1981. Some relationships between the biochemistry of photosynthesis and the gas exchange of leaves. *Planta* **153**: 376–387.

Cernusak LA, Ubierna N, Jenkins MW, Garrity SR, Rahn T, Powers HH, Hanson DT, Sevanto S, Wong SC, McDowell NG *et al.* 2018. Unsaturation of vapor pressure inside leaves of two conifer species. *Scientific Reports* **8**: 1–7.

Cowan IR. 1972. Mass and heat transfer in laminar boundary layers with particular reference to assimilation and transpiration in leaves. *Agricultural Meteorology* **10**: 311–329.

Cowan IR. 1986. *Economics of carbon fixation in higher plants.* Cambridge, UK: Cambridge University Press, 133–170.

Enns T. 1967. Facilitation by carbonic anhydrase of carbon dioxide transport. *Science* **155**: 44–47.

Evans JR. 2021. Mesophyll conductance: walls, membranes and spatial complexity. *New Phytologist* **229**: 1864–1876.

Evans JR, Kaldenhoff R, Genty B, Terashima I. 2009. Resistances along the CO_2 diffusion pathway inside leaves. *Journal of Experimental Botany* **60**: 2235–2248.

Evans JR, Vogelmann TC. 2003. Profiles of ^{14}C fixation through spinach leaves in relation to light absorption and photosynthetic capacity. *Plant, Cell & Environment* **26**: 547–560.

Evans JR, von Caemmerer S. 1996. Carbon dioxide diffusion inside leaves. *Plant Physiology* **110**: 339–346.

Farquhar GD, Busch FA. 2017. Changes in the chloroplastic CO_2 concentration explain much of the observed Kok effect: a model. *New Phytologist* **214**: 570–584.

Farquhar GD, Raschke K. 1978. On the resistance to transpiration of the sites of evaporation within the leaf. *Plant Physiology* **61**: 1000–1005.

Farquhar GD, von Caemmerer S, Berry JA. 1980. A biochemical model of photosynthetic CO_2 assimilation in leaves of C_3 species. *Planta* **149**: 78–90.

Furukawa A. 1992. Ontogenetic changes in stomatal size and conductance of sunflowers. *Ecological Research* **7**: 147–153.

Gaastra P. 1959. *Photosynthesis of crop plants as influenced by light, carbon dioxide, temperature, and stomatal diffusion resistance.* Wageningen, the Netherlands: Mededeling Landbouwhogeschool.

Hanson D, Stutz SS, Boyer JS. 2016. Why small fluxes matter: the case and approaches for improving measurements of photosynthesis and (photo) respiration. *Journal of Experimental Botany* **67**: 3027–3039.

Harley PC, Loreto F, Di Marco G, Sharkey TD. 1992. Theoretical considerations when estimating the mesophyll conductance to CO_2 flux by analysis of the response of photosynthesis to CO_2. *Plant Physiology* **98**: 1429–1436.

Holloway-Phillips M, Cernusak LA, Stuart-Williams H, Ubierna N, Farquhar GD. 2019. Two-source $\delta^{18}O$ method to validate the $CO^{18}O$-photosynthetic discrimination model: implications for mesophyll conductance. *Plant Physiology* **181**: 1175–1190.

Jarvis PG, Slatyer RO. 1966. *A controlled-environment chamber for studies of gas exchange by each surface of a leaf.* Melbourne, Vic., Australia: Commonwealth Scientific and Industrial Research Organization.

Jones H, Slatyer R. 1972. Effects of intercellular resistances on estimates of the intracellular resistance to CO_2 uptake by plant leaves. *Australian Journal of Biological Sciences* **25**: 443–454.

Lamour J, Davidson KJ, Ely KS, Li Q, Serbin SP, Rogers A. 2021. New calculations for photosynthesis measurement systems: what's the impact for physiologists and modelers? *New Phytologist* **233**: 592–598.

Lei ZY, Han JM, Yi XP, Zhang WF, Zhang YL. 2018. Coordinated variation between veins and stomata in cotton and its relationship with water-use efficiency under drought stress. *Photosynthetica* **56**: 1326–1335.

Li-Cor B. 2020. *Using the LI-6800 v.1.4.* Lincoln, NE, USA: Li-Cor.

Long SP, Farage PK, Bolhár-Nordenkampf HR, Rohrhofer U. 1989. Separating the contribution of the upper and lower mesophyll to photosynthesis in *Zea mays* L. leaves. *Planta* **177**: 207–216.

Márquez DA, Stuart-Williams H, Farquhar GD. 2021a. An improved theory for calculating leaf gas exchange more precisely accounting for small fluxes. *Nature Plants* **7**: 317–326.

Márquez DA, Stuart-Williams H, Farquhar GD, Busch FA. 2021b. Cuticular conductance of adaxial and abaxial leaf surfaces and its relation to minimum leaf surface conductance. *New Phytologist* **233**: 156–168.

Mizokami Y, Oguchi R, Sugiura D, Yamori W, Noguchi K, Terashima I. 2022. Cost–benefit analysis of mesophyll conductance: diversities of anatomical, biochemical and environmental determinants. *Annals of Botany.* **130**: 265–283.

Moss DN, Rawlins SL. 1963. Concentration of carbon dioxide inside leaves. *Nature* **197**: 1320–1321.

Mott KA, Buckley TN. 2000. Patchy stomatal conductance: emergent collective behaviour of stomata. *Trends in Plant Science* **5**: 258–262.

Mott KA, O'Leary JW. 1984. Stomatal behavior and CO_2 exchange characteristics in amphistomatous leaves. *Plant Physiology* **74**: 47–51.

Nascimento ÂMP, Reis SN, Nery FC, Curvelo ICS, Taques TC, Almeida EFA. 2016. Influence of color shading nets on ornamental sunflower development. *Ornamental Horticulture* **22**: 6.

Parkhurst DF. 1994. Diffusion of CO_2 and other gases inside leaves. *New Phytologist* **126**: 449–479.

Parkhurst DF, Wong SC, Farquhar GD, Cowan IR. 1988. Gradients of intercellular CO_2 levels across the leaf mesophyll. *Plant Physiology* **86**: 1032–1037.

Pearson M, Davies WJ, Manafield TA. 1995. Asymmetric responses of adaxial and abaxial stomata to elevated CO_2: impacts on the control of gas exchange by leaves. *Plant, Cell & Environment* **18**: 837–843.

Pemadasa MA. 1979. Movements of abaxial and adaxial stomata. *New Phytologist* **82**: 69–80.

Pons TL, Flexas J, von Caemmerer S, Evans JR, Genty B, Ribas-Carbo M, Brugnoli E. 2009. Estimating mesophyll conductance to CO_2: methodology, potential errors, and recommendations. *Journal of Experimental Botany* **60**: 2217–2234.

Raven JA, Glidewell SM. 1981. Processes limiting photosynthetic conductance. In: Johnson CB, ed. *Physiological processes limiting plant productivity.* London, UK: Butterworth, 109–136.

Rockwell FE, Holbrook NM, Jain P, Huber AE, Sen S, Stroock AD. 2022. Extreme undersaturation in the intercellular airspace of leaves: a failure of Gaastra or Ohm? *Annals of Botany* **130**: 301–316.

Sharkey TD, Bernacchi CJ, Farquhar GD, Singsaas EL. 2007. Fitting photosynthetic carbon dioxide response curves for C_3 leaves. *Plant, Cell & Environment* **30**: 1035–1040.

Vogelmann TC, Evans JR. 2002. Profiles of light absorption and chlorophyll within spinach leaves from chlorophyll fluorescence. *Plant, Cell & Environment* **25**: 1313–1323.

Wang XQ, Wu WH, Assmann SM. 1998. Differential responses of abaxial and adaxial guard cells of broad bean to abscisic acid and calcium. *Plant Physiology* **118**: 1421–1429.

Wong SC, Canny MJ, Holloway-Phillips M, Stuart-Williams H, Cernusak LA, Márquez DA, Farquhar GD. 2022. Humidity gradients in the air spaces of leaves. *Nature Plants* **8**: 971–978.

Wong SC, Cowan IR, Farquhar GD. 1978. Leaf conductance in relation to assimilation in *Eucalyptus pauciflora* Sieb. ex Spreng: influence of irradiance and partial pressure of carbon dioxide. *Plant Physiology* **62**: 670–674.

Wong SC, Cowan IR, Farquhar GD. 1985a. Leaf conductance in relation to rate of CO_2 assimilation I. Influence of nitrogen nutrition, phosphorus nutrition, photon flux density, and ambient partial pressure of CO_2 during ontogeny. *Plant Physiology* **78**: 821–825.

Wong SC, Cowan IR, Farquhar GD. 1985b. Leaf conductance in relation to rate of CO_2 assimilation II. Effects of short-term exposures to different photon flux densities assimilation. *Plant Physiology* **78**: 826–829.

Wong SC, Cowan IR, Farquhar GD. 1985c. Leaf conductance in relation to rate of CO_2 assimilation III. Influences of water stress and photoinhibition. *Plant Physiology* **78**: 830–834.

Supporting Information

Additional Supporting Information may be found online in the Supporting Information section at the end of the article.

Notes S1 Derivation of c_w from adaxial and abaxial gas exchange measurements.

Notes S2 R script to calculate c_w.

Notes S3 Impact of neglecting small fluxes in vCF equations.

Notes S4 Noble gases data from Wong *et al.* (2022).

Notes S5 Light induction.

Notes S6 Derivation of total g_{sw}, adaxial, and abaxial c_i, c_s, and w_s.

Notes S7 Derivation to estimate w_i.

Notes S8 Estimation of unsaturation.

Table S1 Estimations of c_w for 30 leaves (10 of each species) at conditions of ASD = 1 kPa, c_a = 400 μmol mol^{-1}, and light intensity of 1000 μmol m^{-2} s^{-1}.

Please note: Wiley is not responsible for the content or functionality of any Supporting Information supplied by the authors. Any queries (other than missing material) should be directed to the *New Phytologist* Central Office.